Non-proportional loading for 3-D stress situations in Sequentially Linear Analysis

Pari, Manimaran; Rots, Jan; Hendriks, Max

DOI
10.1201/9781315182964-108

Publication date
2018

Document Version
Final published version

Published in
Computational Modelling of Concrete Structures

Computational Modelling of Concrete Structures – Meschke, Pichler & Rots (Eds)
© 2018 Taylor & Francis Group, London, ISBN 978-1-138-74117-1

Non-proportional loading for 3-D stress situations in sequentially linear analysis

M. Pari & J.G. Rots
Faculty of Civil Engineering and Geosciences, Delft University of Technology, Delft, The Netherlands

M.A.N. Hendriks
Faculty of Civil Engineering and Geosciences, Delft University of Technology, Delft, The Netherlands
Norwegian University of Science and Technology, Trondheim, Norway

ABSTRACT: This article presents a new non-proportional loading strategy for Sequentially Linear Analysis (SLA), which is a robust secant stiffness based procedure for nonlinear finite element analysis of quasi-brittle materials, like concrete and masonry. The strategy is based on finding the principal planes for a total strain based fixed cracking model, by searching for the critical plane where the normal stresses due to the scaled combination of two non-proportional loads is equal to the allowable strength. For a plane stress situation (2D), the scaling factor λ is expressed as a function of θ, the inclination of an arbitrary plane to the reference coordinate system, and a one dimensional (θ) optimization of λ is done to determine the principal plane and the resulting fixed crack coordinate system. This approach has been illustrated to match up to the closed form solution, obtained previously based on the principal stress theory, using single element tests and a quasi-static test pushover test on a masonry shear wall. Finally, the concept for the 3-D stress situation is presented, where the optimization problem becomes two-dimensional, with respect to *l* and *m* (two-directional cosines).

1 INTRODUCTION

The Sequentially Linear Analysis (SLA) procedure is a total approach, in the context of total strain based fixed cracking models, wherein a sequence of scaled linear analyses is performed coupled with decreasing secant stiffness and strength at the critical integration point of a finite element model. In contrast to the traditional incremental-iterative nonlinear finite element analyses, the key aspect of the SLA approach is the departure from using the tangent stiffness, which significantly affects the stability of FE solutions in softening regions, to the secant stiffness which would yield numerically favourable positive definite stiffness matrices. The constitutive law is discretized into the so-called saw tooth laws with decreasing positive secant stiffness and has undergone improvements over the years to have mesh objective results (Rots et al. 2009).

The procedure was initially developed for a proportional loading scheme, where the rate of change of all loads is the same. The extension of SLA to non-proportional loading, closer to real life loading situations, was rather difficult and was initially confined to plane stress situations (2-D) in a fixed cracking model approach. When there are multiple non-proportional loads, problems arise with respect to finding the critical integration point and the scaling of the loads. The approach initially was based on expressing global stresses as the superposition of stresses due to constant and (non-proportional) variable loads. Subsequently, using the principal stress theory, a closed form solution (DeJong et al. 2008) for the critical load multiplier was found and the crack coordinate system was established for the secondary cracking to follow. The Force-release (F-R) method (Elias et al. 2010), another alternative for the non-proportional loading problem, additionally aimed to address the dynamic phenomenon due to a damage event, that could lead to a series of subsequent failures in the vicinity of a damaged element, by redistributing the unbalanced forces gradually. Since it could not handle snap backs because of not being able to alter the previously applied load (constant load), the General method was proposed (Elias 2015) of which the F-R and the load-unload (L-U) methods (like SLA) are extreme cases, depending on time scales for the redistribution. Simultaneously, a constrained maximization analogy with a double load multiplier strategy (Van de Graaf 2017), one for constant and the other for variable loads was also conceived to address the redistribution phenomenon and was illustrated using continuum

models for larger scale simulations like settlement of a building and pushover of masonry walls. This approach is used as reference in this study.

For a 3-D stress situation, as in the case of solid/brick finite elements, a fixed cracking model allowing for 3-D cracking had already been proposed (Voormeeren 2011) in the context of SLA, however, only for a proportional loading scheme. Thus, there was a need for a non-proportional loading strategy suitable for 3-D stress situations in SLA. Using the approach of principal stress evaluation for 3-D stress situations, as done in the plane stress case by DeJong, results in cubic equations in the load multiplier λ and the resulting closed form solution for λ is very complex. Thus, alternatives were sought to avoid the necessity for a closed form solution of the critical load multiplier and this forms the crux of the study.

In this article, we present a new non-proportional loading strategy based on finding the principal planes, and thus the fixed crack coordinate system, by searching for the plane where the normal stresses due to the scaled combination of two non-proportional loads is equal to the allowable strength. This is done by optimization of the critical load multiplier, expressed as a function of the inclination of an arbitrary plane, and the normal stresses on the plane due to a constant and a (non-proportional) variable load.

2 BACKGROUND THEORY

2.1 *General workflow*

The procedure for SLA is as follows:

1. Set up the saw-tooth laws as shown in Figure 1.
2. Run a linear analysis with full value of the constant load.
3. In case of damage already in this stage (nonlinearity):
   a. Identify the critical integration point with the least ratio of (σ_1/f_t), where σ_1 is the maximum principal stress and f_t is the allowable strength.
   b. Scale the constant load.
   c. Reduce the strength and stiffness of the critical integration point based on the saw-tooth law.
   d. Return to step 2 and repeat until the scaled value of the constant load is the same as the original full value.
4. Once the constant load is fully applied, add the variable load as a unit load and perform a linear analysis.
5. Construct the global stresses as a superposition of the stresses due to the constant and variable load (indicated with indices 'c' and 'v' respectively) and find a closed form solution for the critical load multiplier from the principal stress theory (plane stress situation) as shown below:

$$\sigma_{xx} = \sigma_{xx,c} + \lambda^* \sigma_{xx,v} \tag{1}$$

$$\sigma_{xx} = \sigma_{xx,c} + \lambda^* \sigma_{xx,v} \tag{2}$$

$$\sigma_{xx} = \sigma_{xx,c} + \lambda^* \sigma_{xx,v} \tag{3}$$

$$\sigma_{(1,2)}(\lambda) = \frac{1}{2}(\sigma_{xx} + \sigma_{yy}) \pm \sqrt{\frac{1}{4}(\sigma_{xx} - \sigma_{yy})^2 + \sigma_{xy}^2} \tag{4}$$

6. Determine the integration point for which the load multiplier λ is critical. In principle, solving for the inequality $\sigma_{(1,2)}(\lambda) \leq f$, where 'f' is the allowable strength, sets of values of λ per integration point per failure direction are found and the maximum value of the common subset is chosen as the critical λ. In the event of an empty solution set, wherein the stress states in no integration point allows for a constitutively admissible scaled combination of the constant and variable loads, a return to an 'intermediate proportional scheme' is done. The 'last successful load combination' is scaled in a proportional way thereby reducing the constant load and also partly retaining the scaled variable load. (Van de Graaf 2017).
7. Once the critical integration point and load multiplier is determined, scale the stresses and

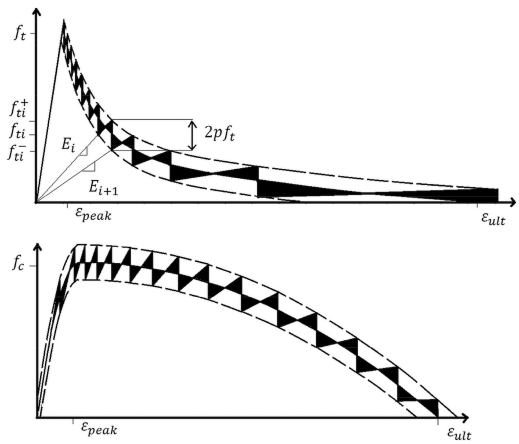

Figure 1. Saw-tooth curves for exponential tension softening (top) and parabolic compressive softening bottom in the ripple curve formulation. The dashed curves represent the delimiting curve at an offset to the 'mother/base' constitutive curve (by a percentage 'p' of the allowable strength) to allow for a formulation with regularized fracture energy to ensure mesh objectivity.

strains as well accordingly and obtain the new stress state.

8. Remove all loads and update the strength and stiffness of the critical integration point based on the saw tooth law and return to step 2 until the element/structure is completely damaged.

2.2 *Fixed cracking model in SLA*

SLA has thus far been based on a total strain based smeared cracking model. As soon as the principal stress violates the allowable strength at an integration point, the isotropic stress strain relation $\sigma = D\varepsilon$, transforms into an orthotropic relation at the *n-t* cracked coordinate system as $\sigma_{nt} = D_{nt}\varepsilon_{nt}$. The normal direction's Young's modulus and strength are damaged according to the saw tooth law. In the event of stress rotations that lead to stresses in the tangential direction violating the allowable strength, the damage is introduced similarly. So every integration point essentially requires two uniaxial saw tooth laws in the 2-D plane stress situation. This aside, the shear behaviour in the fixed cracking model is represented using a variable step wise shear retention function that takes into account the reduction of shear stiffness with increasing damage in normal direction of the cracked plane. Also, the Poisson's ratio is reduced at the same rate as the associated Young's modulus.

2.3 *Motivation for a new non-proportional strategy*

Determining the critical load multiplier in a plane stress situation is straightforward as shown in the previous section. Substitution of the global stresses, i.e. Equation 1, 2, and 3, into the expression for the principal stress (Equation 4), would yield a quadratic equation in λ thereby resulting in a closed form solution. So the existence of a rather simple expression for the principal stress is key to this approach and this is primarily because the characteristic equation for a 2-D stress situation is also a quadratic equation.

However, for a 3-D stress situation the principal stresses would be the roots of a cubic characteristic equation (Equation 7).

$$\det(\Sigma - \Lambda\mathbf{I}) = 0 \tag{5}$$

$$\begin{vmatrix} \sigma_{xx} - \Lambda & \sigma_{xy} & \sigma_{zx} \\ \sigma_{xy} & \sigma_{yy} - \Lambda & \sigma_{yz} \\ \sigma_{zx} & \sigma_{yz} & \sigma_{zz} - \Lambda \end{vmatrix} = 0 \tag{6}$$

$$\Lambda^3 - I_1\Lambda^2 + I_2\Lambda - I_3 = 0 \tag{7}$$

where Σ is the 3-D stress tensor, Λ are the principal values, $\mathbf{I}$ is the Identity matrix and I_1, I_2 and I_3 are the stress invariants. An analytical expression for the principal values from Equation 7 would not be as simple as Equation 4. It is well documented in literature about mathematical procedures like Cardano's method (Birkhoff & MacLane 1997) involving transformation to get reduced cubic equations and subsequent reduction to a quadratic equation to find analytical solutions, but such an approach for solving Equation 7 would prove rather complex and cumbersome. Since the superposed stresses as in Equation 1, 2 and 3 would introduce a new variable λ, finding a closed form solution, to be able to implement in a finite element framework, becomes rather unrealistic.

This motivated the need for a new non-proportional strategy suitable for the 3D stress situations. Numerical algorithms were considered as a possible solution to solve the cubic equation with the additional variable λ, but to reduce the complexity of the problem, reformulation of the problem statement was regarded to be more pragmatic and this led to the new approach described in the next section. The problem is reduced to that of a two-dimensional optimization problem, the directional cosines, in the 3-D case but is first elucidated in the 2-D plane stress situation to match up to the existing closed form solution.

3 REFORMULATION OF NON-PROPOPORTIONAL LOADING IN SLA

3.1 *Concept*

The non-proportional loading strategy being considered retains the concept of superposition of stresses due to the two non-proportional loads, referred to as constant and variable loads hereon, to obtain global stresses. Instead of resorting to the principal stress theory to find the closed form solution for λ, the normal stress on an arbitrary plane is now expressed as a function of the inclination of the plane to the reference axes.

The normal stresses due to the constant and the variable loads (denoted by the subscripts *c* and *v*) would be functions of θ:

$$\sigma_{nn,c} = \frac{1}{2}\left(\sigma_{xx,c} + \sigma_{yy,c}\right) + \frac{1}{2}\left(\sigma_{xx,c} - \sigma_{yy,c}\right)\cos(2\theta) + \sigma_{xy,c}\sin(2\theta) \tag{8}$$

$$\sigma_{nn,v} = \frac{1}{2}\left(\sigma_{xx,v} + \sigma_{yy,v}\right) + \frac{1}{2}\left(\sigma_{xx,v} - \sigma_{yy,v}\right)\cos(2\theta) + \sigma_{xy,v}\sin(2\theta) \tag{9}$$

The scaled combination of the stresses shown, σ_{nn}, above would have to be equal to the allowable strength, from which the load multiplier λ, is expressed as a function of θ as shown below:

$$\lambda(\theta) = (f - \sigma_{nn,c}(\theta)) / \sigma_{nn,v}(\theta) \quad (10)$$

where f is the allowable strength.

The idea is to find the minimum value of λ, at which the slope of the function is zero, and the corresponding value of θ will determine the inclination of the failure (cracking/crushing) plane. This was initially verified for simple stress states by comparing against the analytically derived closed form solution for λ and the inclination of the crack plane as formulated by DeJong et al. (2008).

The function of the load multiplier may be continuous or discontinuous for different stress states but is periodic every π radians. Thus, it is sufficient to evaluate the function over a range of $\theta = [-\pi/2, \pi/2]$ to evaluate the critical λ and the corresponding critical cracking plane. Typical functions are shown in Figure 3.

It is observed that the maxima or minima of this function correspond to 'critical' values of λ for which the scaled combination of the normal stresses due to constant and variable loads, σ_{nn}, approach the allowable strength. The physical meaning of the expression for λ as a function of the cracking inclination θ is that there several combinations of λ and θ for a certain kind of loading (stress state). However, there are only two critical admissible values in the interval $\theta = [-\pi/2, \pi/2]$, the maxima and the minima, for a certain stress state which could be seen as upper and the lower bound

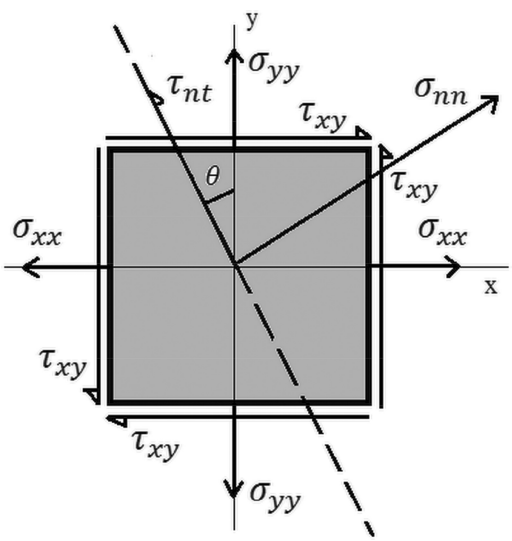

Figure 2. Plane stress situation: Normal stress σ_θ and Shear stress τ_θ, on a plane at an inclination θ to the reference axes.

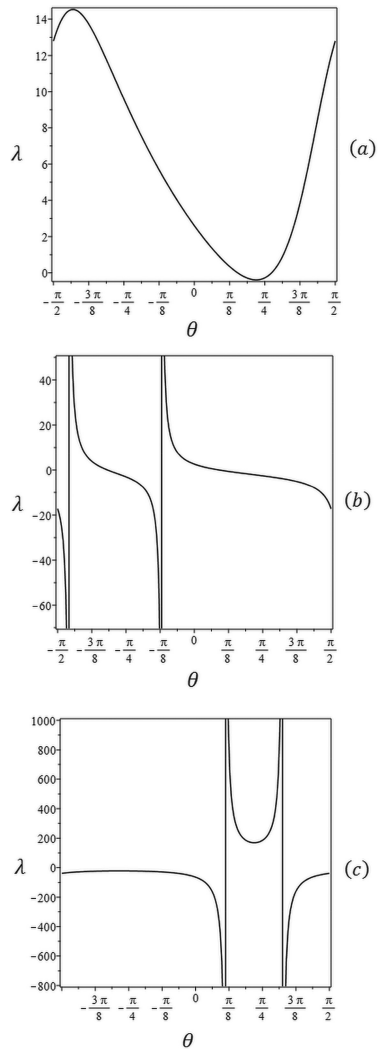

Figure 3. Example of functions of λ with respect to the inclination of an arbitrary plane at an inclination θ to the reference axes where: (a) there are global critical points, (b) there are 'no' critical points (infinite real set) and (c) there are local critical points, that can result in a possible load combinations to initiate failure.

solutions. These bounds are analogous to the λ_{min} and λ_{max} of the sets of admissible lambda values found per integration point as described by Van de Graaf (2017). Therefore, along the same lines, the critical values for each integration point are used to set up the 'sets' of λ values, and the maximum of the common subset is chosen as the global critical load multiplier λ_{crit}. In the event of an empty common subset, the strategy to temporarily reduce the constant load by proportionally scaling the 'last

successful' load combination as mentioned in section 2.1 is adopted (Van de Graaf 2017).

In case of functions such as those shown in Figure 3(b), there appears to be only global extreme values at certain θ and no local critical points. This would mean that critical bounding solutions where failure can be initiated are infinite and so such cases can be neglected. In other words, the range of admissible values of the scaled variable load to initiate failure at an integration point is the infinite real set.

Additionally, it is to be noted that for the new crack coordinate system at an inclination θ with respect to the reference coordinate system, there will also be a normal stress σ_{tt} which is not to be neglected. For the critical λ evaluated by finding the optimum θ with respect to σ_{nn}, the corresponding σ_{tt} at an angle (θ +π/2) should be lesser than the maximum principal stress or greater than minimum principal stress, for tensile or compressive failure along σ_{nn} respectively. Thereby we ensure that the derived λ also results in the normal stresses which are in accordance to the principal stress theory. Depending on these aspects of the function, we can address the non-proportional loading strategy now as an optimization problem.

3.1.1 *Minimization of the λ function using optimization algorithm*

With the knowledge of typical functions within the interval [–π/2, π/2], the choice to utilize optimization techniques, to find the minimum for every integration point per linear analysis, was made. In this study, the minimization of the function is carried out in two stages if the function is smooth and parabolic near the minima as shown in Figure 3(a) and Figure 3(c). Firstly, the minimum is bracketed using the inverse parabolic interpolation. Subsequently, the golden section search algorithm (Kiefer 1953) is used to find a functional minimum. This method is the optimization counterpart of the root finding bisection method. The idea is to successively narrow down the set of values to a small interval where the minimum exists. The convergence towards the minimum is linear but the method is always guaranteed to converge. The maximum can be found by adopting the same strategy but with the negative of the function. In scenarios wherein no minima occurs as shown in Figure 3(b) or there are global minimum (extreme values) alongside the critical local minimum as in the case of Figure 3(c), the algorithm has to be modified, to appropriately find the critical points or neglect the integration point with such stress states on the whole. The knowledge of the first derivative of the function can make it possible to use faster optimization routines to find the desired critical points and this is being currently investigated. Nevertheless, as explained in the following sections, the strategy matches up to the existing closed-form solution based strategy and also in terms of computational effort (time).

4 VALIDATION STUDIES (2D)

4.1 *Single element test*

The concept for the reformulated non proportional strategy, hereon referred to as the Sequentially linear 'theta-based' non-proportional strategy (SLTHNP) was implemented and validated in the commercial FEA program DIANA FEA. Several single element tests were performed and one such is presented in this paper. The scheme of the test on the linear plane stress element is as shown in Figure 4. The plane stress element is assigned unit material properties as shown in Table 1. The test is performed with both the SLTHNP and the closed

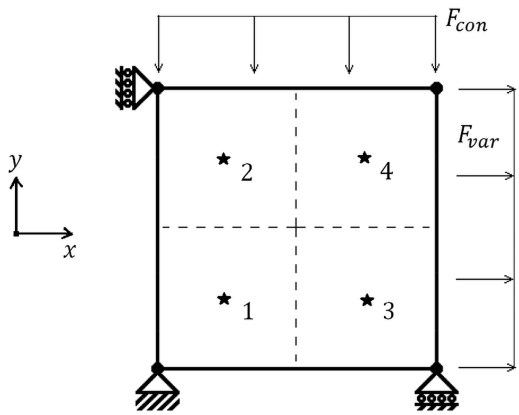

Figure 4. A Linear plane stress element, with boundary conditions as shown, is subject to constant load F_{con} in the negative-y direction followed by the unit proportional load F_{var} in the positive-x direction. In-plane Gaussian integration scheme 2 × 2 is used (demarked as stars).

Table 1. Material properties for the test.

Property	Value	Units
Young's Modulus (E)	1000	N/m²
Poisson's ration (*v*)	0	–
Tensile strength (f_t)	1	N/m²
Tensile Mode-I fracture energy (G_{fI})	1	N/m
Compressive strength (f_c)	1	N/m²
Compressive fracture energy (G_c)	1	N/m
Number of Saw-tooth*	20	–

*Linear Tensile and parabolic compressive Saw-tooth as shown in Figure 1 with a 'p' factor of 0.1.

form solution based non-proportional strategy of DeJong later improved by Van de Graaf (2017), hereon referred to as SL2DNP.

The constant load is kept low to about 0.01 N/m so that damage in an integration point happens only when the variable load is applied and the non-proportional loading strategy, as the case may be, determines the cracking plane and the load multiplier. The stress strain evolution in all 4 integration points is observed for both simulations with SL2DNP and SLTHNP.

Since the loading is such that damage will occur only in tension along the X-direction, the corresponding stress strain relations in X-direction alone are presented in Figure 5. It can be seen for integration points 1 and 2 that at certain load steps an integration point may lie on the secant branch (as another point becomes critical) or at the upper limit point of the saw tooth, depending on whether or not the point under consideration is critical, and vice versa. As expected, in line with similarities observed for simple stress states as mentioned in the previous section (analytical comparisons), the approaches match. A similar test with constant tension load in Y (but small enough to avoid damage) and the variable compression load in X directions also show good agreement between the approaches. This validates the SL2DNP at element level but there was need for an assessment at a structural level involving stress redistributions and this is shown in the next section.

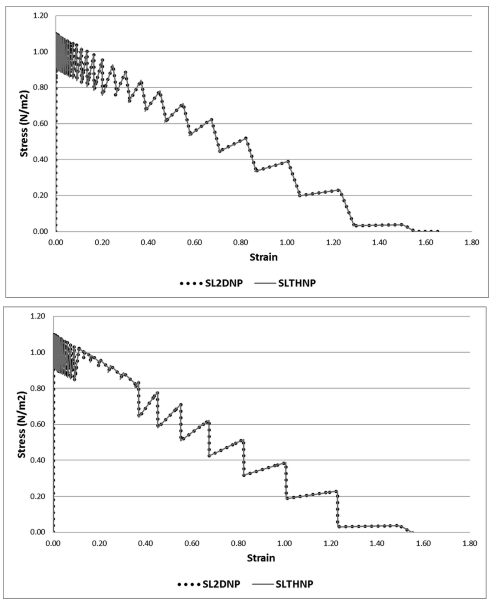

Figure 5. Stress strain evolution along the x-direction which is subject to tension as observed using the closed form solution based SL2DNP strategy and the theta based new SLTHNP strategy for integration points 1 & 2 - (top) and (bottom) respectively.

4.2 *Quasi-static cyclic pushover test—High wall*

To demonstrate the SLTHNP strategy, the benchmark of a calcium silicate masonry shear wall test is chosen. Several in-plane quasi-static cyclic tests were performed on calcium-silicate and clay brick walls at TU Delft in the Stevin Lab as a part of the extensive research campaign addressing the induced seismic situation in Groningen, The Netherlands (Rots et al. 2016). Of these, one of the high walls is tested using SLA with the SL2DNP and SLTHNP strategies.

The constitutive relationship combining a linear tension softening and a parabolic compression softening behaviour in uniaxial direction, similar to that presented in Figure 1, is used. The wall is slender, around 2.75 m × 1.1 m in size. It is a single wythe wall of thickness 0.1 m and is subject to a vertical precompression of 0.7 MPa. The experimental setup has double clamped boundary conditions (top edge remains straight but is free to move vertically in the direction of overburden). After application of precompression, a lateral load is applied in a cyclic fashion. The experimental setup is shown in Figure 6 and the end stage damage pattern was a combination of flexure (rocking failure), toe crushing and sliding failures. For further details refer Ravenshorst et al. (2016). Although the test is cyclic in nature, the test could be used as a benchmark in a monotonic approach to make qualitative comparisons between the experimental backbone/envelope curve and the SL2DNP and SLTHNP non-proportional strategies.

The force displacement curves from the SL2DNP and SLTHNP simulations, in comparison

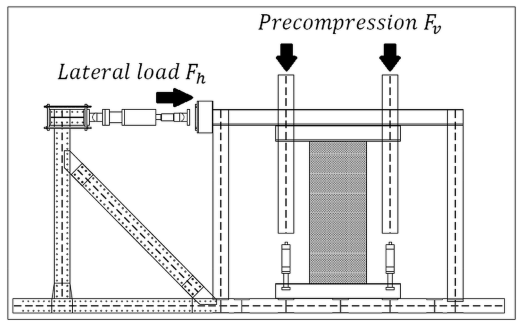

Figure 6. Experimental setup of shear wall with dimension 2.75*1.1 m^2 with thickness 0.102 m. The pre-compression and lateral loads are applied using hydraulically controlled actuators as shown (Ravenshorst et al. 2016).

to the experimental backbone curve are shown in Figure 8. There is a slight deviation in the numerical result from the experiment and this can attributed to calibration of material properties which were obtained from material level tests which were also done as a part of the campaign. These are shown in Table 2.

Nevertheless, the aim of the study is to demonstrate the applicability of the proposed non-proportional strategy for Sequentially linear analysis and therefore in-depth comparisons are made only between the SL2DNP and SLTHNP approaches and only an overall/global comparison to the experimental benchmark in terms of the damage patterns and the failure modes is made. For the same reasons, the comparison between the approaches is stopped at 7.0 mm for the simulations while the experiment was continued to around 25 mm top displacement.

The results from both the simulations are in agreement until the top displacement of 7.0 mm until which the analysis has been investigated. Since the results from SL2DNP match exactly with those from SLTHNP, the evolution of the maximum principal strain ε_1 is shown only for the SLTHNP simulations in Figure 7. The rocking/flexure failure that was observed in the experiment is seen in both simulations and the strain contours are in agreement.

However, there are a couple of points to be noted. The optimization routine to find critical λ, the golden search algorithm, is dependent on a certain tolerance for convergence to the solution and the solution is sensitive to this parameter. Varying the tolerance further may alter the proximity to the closed form solution; however beyond a certain value this would not be the case. The sensitivity of the SLTHNP with respect to this tolerance is currently being investigated with this benchmark and the one discussed in the next section.

It has to be pointed out that compressive softening was not observed for the displacements considered. This is due to the choice of comparing simulations until a net top displacement of 7.0 mm. Also, the combined tension-compression biaxial failure model that has been used in this study has an intrinsic problem that in a uniaxial case, if an integration point softening in tension unloads locally (is possible for monotonic analysis also due to stress redistributions (Van de Graaf 2017)) it carries over the damaged stiffness into compressive regime and this could affect the results. This aspect of the biaxial failure envelope is also being currently investigated.

4.3 *Quasi-static cyclic pushover test—Low wall*

The benchmark presented in the previous section exhibits a rather simple damage pattern, a rocking mode. In order to authenticate the validity of the SLTHNP strategy in comparison to SL2DNP for another failure mode, the benchmark of low wall that exhibited a brittle failure by diagonal cracking is investigated.

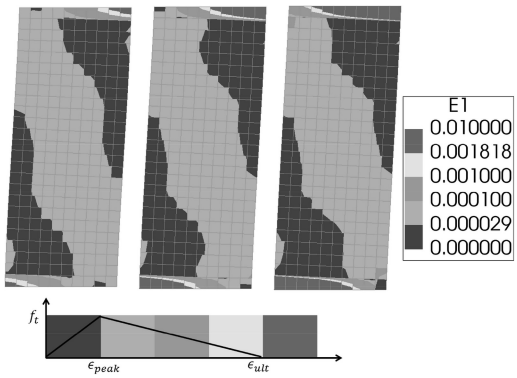

Figure 7. Maximum principal strain ε_1 evolution at A, B and C points of Figure 8 for SLA using SLTHNP non-proportional loading strategy.

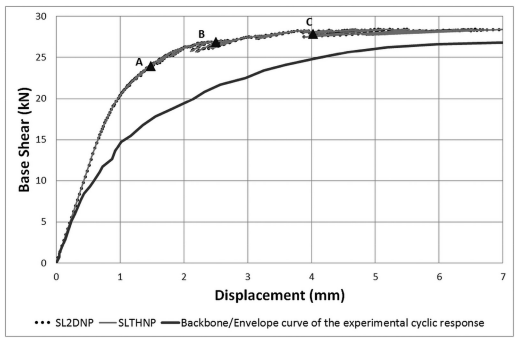

Figure 8. Comparison of the monotonic SLA simulations of the shear wall test using SL2DNP and SLTHNP non-proportional loading strategies and the envelope curve of the cyclic experimental curve.

Table 2. Material properties for the shear wall test *.

Property	Value	Units
Young's Modulus (E)	5.091E+09	N/m^2
Poisson's ration (v)	0.2	–
Tensile strength (f_t)	0.15E+06	N/m^2
Tensile Mode-I fracture energy (G_{fI})	15	N/m
Compressive strength (f_c)	5.93E+06	N/m^2
Compressive fracture energy (G_c)	31300	N/m
Number of Saw-tooth	30	–

*Properties obtained from material level tests on calcium silicate masonry (Esposito et al. 2016).

The wall considered is rather squat in comparison to the previous benchmark, around 1.35 m(high) × 1.1 m in size. The experimental setup has double clamped boundary conditions and after application of precompression of 0.6 MPa, a lateral load is applied in cyclic fashion similar to the previous benchmark. The experimental setup is shown in Figure 9. The material properties for the constitutive relationship combining a linear tension softening and a parabolic compression softening behaviour in uniaxial direction, similar to that presented in Figure 1, is presented in Table 3.

The only point to be noted is that the elements in the middle of the wall in Figure 9 are assigned a higher Mode-I fracture energy than the extreme row of elements (grey-coloured) in order to account for the relatively larger energy dissipation in a shear failure as against a rocking failure. Diagonal shear failure was observed in the experiment subsequent to reaching the peak force. For further details about the experiment refer Anthoine et al. (1995). Monotonic simulations are made to make qualitative comparisons between the SL2DNP and SLTHNP non-proportional strategies.

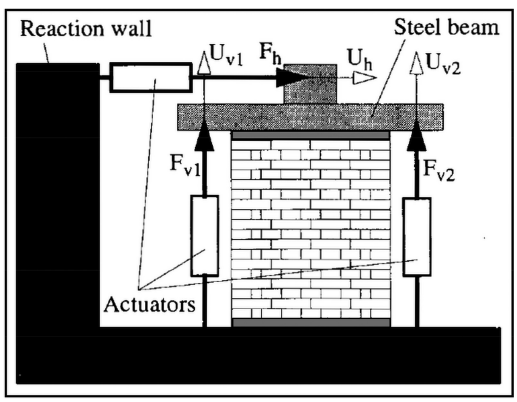

Figure 9. Experimental setup of low-shear wall, Anthoine et al. (1995).

Table 3. Material properties for low-wall test*.

Property	Value	Units
Young's Modulus (E)	1.491E+09	N/m^2
Poisson's ration (ν)	0.15	–
Tensile strength (f_t)	0.15E+06	N/m^2
Tensile Mode-I fracture energy (G_{fI})	150	N/m
Compressive strength (f_c)	6.20E+06	N/m^2
Compressive fracture energy (G_c)	40000	N/m
Number of Saw-tooth	30	–

*Properties calibrated after sensitivity analysis for tensile mode-I fracture energy and tensile strength. Additionally for continuum elements (extreme rows) G_{fI} = 100 N/m.

The results from the SLTHNP and SL2DNP simulations exactly match thereby validating the new strategy for the non-proportional loading problem. In contrast to the previous benchmark, here a return to the 'intermediate proportional scheme' proposed by Van de Graaf (2017) is also

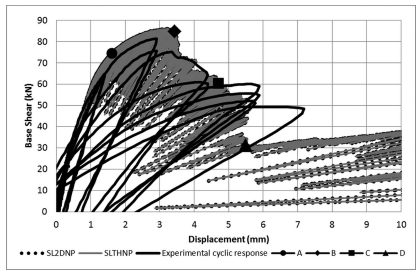

Figure 10. SL2DNP and SLTHNP simulations of the low wall test and the characteristic points A, B, C and D.

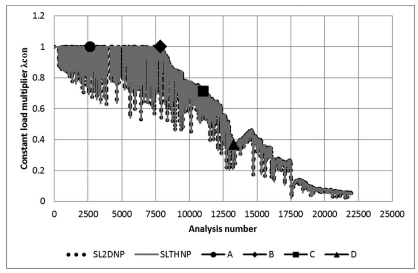

Figure 11. Evolution of λ_{con} in the two simulations of the low wall test and the characteristic points from Figure 10.

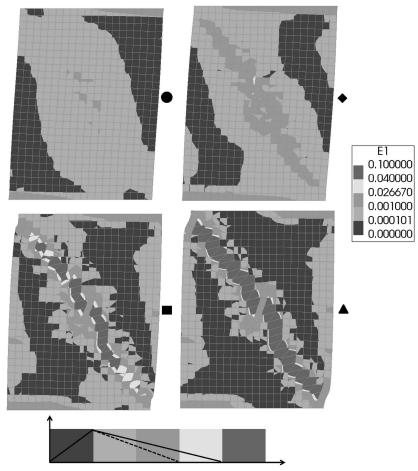

Figure 12. Evolution of principal strain 1 (dotted softening branch—extreme elements, whole—middle elements).

observed. This is seen in Figure 11, where the load multiplier associated with the constant load (in this case the precompression) λ_{con} reduces below 1.0 over the number of linear analysis steps. It regains the initial value of precompression most often but post step 7850, there seems to be a gradual decrease up until step 13300 where the value reaches almost 0.3. Physically this would mean that the precompression on the wall cannot be recovered and the gradual decrease could be interpreted as the wall nearing collapse state. Damage pattern for 4 characteristic points A, B, C and D in Figure 10 are shown in Figure 12 and a comparison between damage patterns of both approaches (exact match) is not made here owing to triviality.

5 EXTENSION OF THE NEW NON-PROPORTIONAL LOADING STRATEGY TO 3-D STRESS SITUATIONS

5.1 *Concept*

The purpose of introducing and demonstrating the theta based non-proportional strategy at a 2-D level was to prove the validity of the method. However, the aim of the strategy is ultimately to have 3-D SLA simulations with non-proportional loading or in other words simulations with a constant and variable load. Due to the aforementioned problems with finding closed form solution in a 3-D stress situation, in line with the 2-D reformulation of the non-proportional problem based on theta—the inclination of the arbitrary plane to the reference axes, the 3-D non-proportional loading problem is reformulated based on directional cosines.

In the 3-D stress situation, an arbitrary plane can be related to the reference coordinate system by means of the directional cosines *l*, *m* and *n*, of which only two may be considered independent variables since they are related as $l^2 + m^2 + n^2 = 1$. The normal stresses acting on this plane due to the constant and variable loads can thus be expressed as

$$\sigma_{nn,c} = \sigma_{xx,c} l^2 + \sigma_{yy,c} m^2 + \sigma_{zz,c} n^2 + (2\sigma_{xy,c} lm) + (2\sigma_{yz,c} mn) + (2\sigma_{xz,c} nl) \quad (11)$$

$$\sigma_{nn,v} = \sigma_{xx,v} l^2 + \sigma_{yy,v} m^2 + \sigma_{zz,v} n^2 + (2\sigma_{xy,v} lm) + (2\sigma_{yz,v} mn) + (2\sigma_{xz,v} nl) \quad (12)$$

The load multiplier is now expressed as a function of only two of the directional cosines, rewriting the third as $n = \sqrt{(1 - l^2 - m^2)}$, as shown below:

$$\lambda(l,m) = (f - \sigma_{nn,c}(l,m)) / \sigma_{nn,v}(l,m) \quad (13)$$

The idea is to find the critical values of λ, the maxima or minima of this function, at which the slope of the function is zero, make sets of admissible values of λ per integration point and choose the maximum λ of the common subset similar to the 2D case. The values of *l*, *m* and *n* corresponding to the λ_{crit} will determine the inclination of the failure (cracking/crushing) plane. The function of the load multiplier may be continuous or discontinuous for different stress states similar to those observed in the 2-D plane stress situation and are shown in Figures 13 and 14. Additionally, analogous to the 2-D case, for the new crack coordinate system at an inclination *l*, *m* and *n,* with respect to the reference coordinate system, there will also be a normal stress σ_{tt} and σ_{ss} which are to be considered. For the critical λ evaluated by finding the optimum *l*, *m* and *n*, with respect to σ_{nn}, the corresponding σ_{tt} and σ_{ss} should be such that $\sigma_1 > \sigma_2 > \sigma_3$.

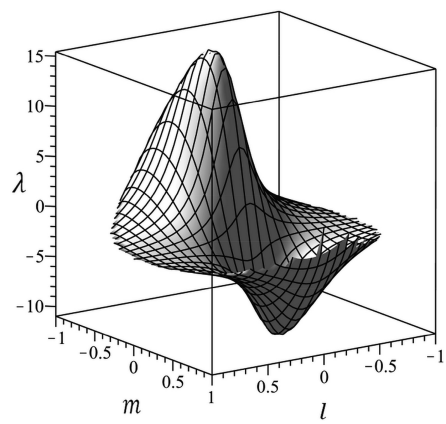

Figure 13. Example of a smooth continuous function of λ with respect to the inclination of an arbitrary plane defined by directional cosines *l* and *m*.

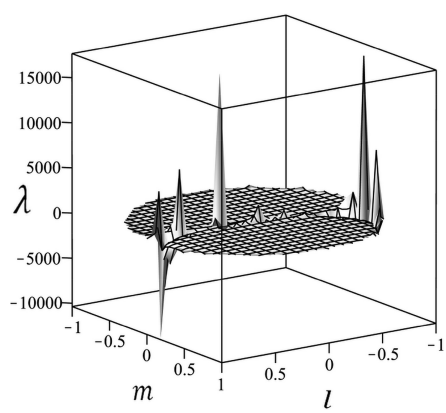

Figure 14. Example of a discontinuous λ with respect to the inclination of an arbitrary plane at an inclination defined by directional cosines *l* and *m*.

In addition to the non-proportional loading strategy the fixed crack approach for the 3-D stress situation to allow for an additional tertiary cracking is necessary. The idea for the change from isotropic to orthotropic formulation upon damage in 2D plane stress situation were extended to the 3D-stress state by Voormeren (2011). Here the transformation of the original isotropic formulation into the *n*-s-*t* orthotropic formulation expressed as $\sigma_{nst} = D_{nst}\ \varepsilon_{nst}$, allowing for tertiary cracking as well, is done. The associated variable shear retention functions and poisson ratio reductions were also considered. The damaged integration point will have 3 each of Young's moduli, shear moduli and poisson's ratio.

The extrema (bounds) of the critical load multiplier was determined in the 2-D stress situation numerically using a one-dimensional optimization routine. In the reformulated 3-D non-proportional loading problem, the optimization has to be done with respect to 2 variables *l* and *m*. So a multidimensional optimization routine is required and preliminary investigations have been made with the rather basic downhill simplex method, the 3-D version of the golden section search. The limitation in multi-dimensional optimization is that the initial bracketing of the extremum is not possible and emphasis has to be laid on possibly restarting the optimization routine from a 'converged solution' repeatedly to ensure that the extremum is indeed global and not a local one. Investigations are also ongoing for the choice of a faster optimization routine like the Conjugate gradient method.

6 CONCLUSIONS

A new strategy for Sequentially linear analysis with a view to address the 3-D non-proportional loading has been presented in this study. This was motivated by the lack of a simple closed form expression for the critical load multiplier λ in the 3-D case as in the 2-D plane stress situation. The problem statement for non-proportional loading has been proposed to be reformulated to first express the normal stress on an arbitrary plane, at an inclination θ with respect to the reference coordinate system, as the scaled combination of the normal stresses due to the constant and variable loads. This was equated to the allowable strength based on the saw-tooth constitutive law and ultimately the load multiplier was expressed as a function of θ. It has been shown in this study that the θ corresponding to extreme/critical values of the aforementioned function would result in inclination of the principal planes, using an optimization routine. First, the approach was presented for a 2-D stress situation and demonstrated using single element tests and quasi-static pushover tests on a slender calcium silicate masonry wall and a squat brick masonry wall. It has been shown to be in agreement with the closed form solution based non-proportional loading strategy as presented by DeJong (2008) and later readapted by Van de Graaf (2017). Furthermore, the concept for the 3-D stress situation has been presented and is currently being investigated with single element tests and benchmarks. Also investigations are ongoing to improve the biaxial tension compression failure model used in this study, to address the crack closure problem; and to extend SLA to cyclic loading applications.

ACKNOWLEDGEMENTS

The research is funded as a part of the author's PhD Program by Nederlandse Aardolie Maatschappij B.V. (NAM) and is gratefully acknowledged. Also, the author is thankful for the contribution of DIANA FEA towards the development of SLA and the additional new implementations.

REFERENCES

Anthoine, A., Magonette, G. & Magenes, G. 1995. Shear compression testing and analysis of brick masonry walls. *10th European conference on earthquake Engg.,* Balkema.

Birkhoff, G. & Maclane, S. 1997. A survey of Modern Algebra. 5th edition, London: A.K. Peters.

DeJong, M.J., Hendriks, M.A.N. & Rots, J.G. 2008. Sequentially linear analysis for fracture under non-proportional loading. *Engineering Fracture Mechanics,* 75, 5042–5056.

Elias, J., Frantik, P. and Vorechovsky, M. 2010. Improved sequentially linear solution procedure. *Engineering Fracture Mechanics,* 77, 2263–2276.

Elias, J. 2015. Generalization of load-unload and force-release sequentially linear methods. *International Journal of Damage Mechanics,* 24(2), 279–293.

Esposito, R., Messali, F., Crielaard R., Rots, J.G. 2016. Tests for the material characterization of replicated masonry and wall ties, *Final Report*, Delft University of Technology.

Kiefer, J. 1953. Sequential minimax search for a maximum. *Proc. American Mathematical Society*, 4 (3): 502–506.

Ravenshorst, G., Messali, F., 2016a. In-of-plane tests on replicated masonry walls. *Final report*, Delft University of Technology.

Rots, J.G., Belletti, B. & Invernizzi, S. 2004. Robust modelling of RC structures with an "event-by-event" strategy. *Engineering Fracture Mechanics,* 75, 590–614.

Rots, J.G, Messali, F., Esposito, R., Jafari, S. & Mariani, V. 2016. Computational modelling of masonry with a view to Groningen induced seismicity. *Proc. of the International conference on SAHC*, Leuven, Belgium.

Van de Graaf, A.V. (2017). Sequentially linear analysis for simulating brittle failure. PhD thesis, Delft University of Technology.

Voormeeren, A.V. (2011). Extension and verification of sequentially linear analysis to solid elements. Master's thesis, Delft University of Technology.